

Single-molecule approach to dispersed kinetics and dynamic disorder: Probing conformational fluctuation and enzymatic dynamics

X. Sunney Xie

Department of Chemistry and Chemical Biology, Harvard University, Cambridge, Massachusetts 02138

(Received 23 September 2002; accepted 27 September 2002)

This article reviews our efforts in understanding dynamical fluctuations of both conformation and enzymatic reactivity in single biomolecules. The single-molecule approach is shown to be particularly powerful for studies of dispersed kinetics and dynamic disorder. New single-molecule observations have revealed conformational transitions occurring on a broad range of timescales, 100 μ s–10 s, offering new clues for understanding energy landscape of proteins, as well as the structural and chemical dynamics therein. © 2002 American Institute of Physics.
[DOI: 10.1063/1.1521159]

I. INTRODUCTION

Perhaps the most profound contribution of the single-molecule approach to biophysical chemistry or even chemical biology is the ability to record movies of molecular motions and to follow the chemical activities of individual macromolecules or their complexes. This is particularly important in the post-genome era when structural biology has yielded a vast amount of information about the structures of biomolecular machineries. When the first structural models of proteins became available, Jeremy Knowles, a renowned enzymologist now at Harvard, observed that “making a model of a horse from photographs does not necessarily tell us how fast it can run.”¹ While structural information is essential, the dynamics are important to the understanding of functions. The famous 1878 fast photography of a running horse by Eadweard Muybridge, the father of motion pictures, pointed to the obvious importance of motion pictures in observing dynamics.² The advent of ultrafast spectroscopy has allowed monitoring of molecular motions with femtosecond time resolution.³ However, these experiments have been conducted with large ensembles of molecules and often require coherent motions of the molecules. Such coherence is created by short laser pulses and is only maintained on the subpicosecond time scale, an event comparable to a pack of racehorses leaving the gate. Under this condition, ensemble-averaged dynamics is identical to single-molecule dynamics. At longer time scales, however, the coherence is lost. This corresponds to a situation where different horses have different actions at different times. Most enzymatic reactions occur at the time scales of millisecond to second, at which molecules do not evolve synchronously. Single-molecule experiments circumvent the necessity of synchronization of many molecules, and provide detailed dynamical information hidden in ensemble-averaged experiments.

Molecular dynamics (MD) simulations are virtual single-molecule experiments that provide vivid movies of molecular motions. MD has substantially enhanced our knowledge of macromolecular dynamics.⁴ Unfortunately, the accessible time scale of MD has been limited to microseconds,⁵ while the actual motions of a biomolecule span from femtoseconds

to seconds or longer. It has been argued that the ultrafast conformational dynamics probed by MD simulations to date have little functional importance besides a few fast photochemical reactions such as the vision process or primary events of photosynthesis, and only the energetics probed by MD is of biochemical importance.⁶ On a single-molecule basis, the event of a chemical reaction occurs on a subpicosecond time scale. However, the waiting time for the reaction to occur is usually much longer because of the low probability for acquiring enough energy to reach the transition state. The subpicosecond conformational dynamics only affects the short-lived transition state and determines the transmission coefficient in transition state theory.^{7,8} It has been well established that dynamics beyond the MD simulation time scale, such as conformational gating of chemical reactions and conformational changes triggered by either ligand binding or chemical reactions is crucially important to macromolecule functions. However, for the reason described above, it has been difficult to study the slow conformational changes in ensemble-averaged experiments. Single-molecule experiments allow the study of these motions and their influence on chemical reactions at a greater level of detail.

With the advent of a variety of single-molecule techniques, movies or trajectories of single enzyme molecules at work have been recorded for many enzymatic systems.^{9–17} More and more single-molecule assays are being developed. Some of these assays are easier or better than the ensemble-averaged assays, while others have no ensemble-averaged equivalents. It is fair to say that, due to the efforts of many groups, the single-molecule approach has changed the way not only biophysical but also biochemical problems are addressed. New insights derived from the single-molecule approach continue to emerge.

The hallmark of the single-molecule movies or trajectories is the ability to capture transient intermediates, which are difficult to detect in ensemble-averaged experiments because of their low concentrations. In some cases, rather long-lived intermediates, such as RNA folding intermediates,¹⁴ can be observed through their spectroscopic identities; in other cases, the existence of the intermediates in enzymatic

reactions, such as the Michaelis–Menten intermediates¹² or those involved in ATP hydrolysis,¹¹ cannot be detected directly because of the lack of observables, but can be inferred from the statistical analyses of single-molecule trajectories. A short review article on this subject has appeared.¹⁸

Another emerging contribution of single-molecule research is the study of conformational fluctuations at enzymatically relevant time scales and their influence on biochemical reactions. Observations of conformation fluctuation are made through optical measurements such as spectral diffusion of emission spectra,¹² fluorescence resonance energy transfer,¹⁹ and photo-induced electron transfer.²⁰ This is a subject related to the long-standing issues of disperse kinetics and dynamic disorder.²¹ In this article, we give a survey of the phenomenon of dynamic disorder associated with conformational fluctuation and the new information extractable from single-molecule experiments.

II. DISPERSED KINETICS AND DYNAMIC DISORDER

Dispersed kinetics exists for many condensed-phase systems, biological systems in particular. A well-known example is the ligand-recombination kinetics of myoglobin following photodissociation.^{22–25} Dispersed kinetics has also been observed in ion channels^{26,27} using the patch clamp technique,²⁸ the first single-molecule technique. Ensemble-averaged experiments often report multiexponential population decays. However, given more than three exponentials, it is difficult to distinguish them in practice. The stretched exponential, known as Kohlrausch–Williams–Watts function, is a phenomenological fitting function in the form of $\exp[-(t/\tau_0)^\gamma]$. It was first used to describe mechanical creep in glassy fibers,²⁹ and more than a century later adapted to describe dielectric constants of glassy and polymeric materials.³⁰ The universality of the stretched exponential in nature has been a subject of extensive inquiry.^{31–33} Practically, the stretched exponential function conveniently describes the dynamics spanning a broad range of time scales with only two adjustable parameters instead of numerous exponentials.

Let us consider a population decay, such as that of an excited fluorophore in protein, or that of an enzyme–substrate complex undergoing a catalytic reaction. Concrete examples of both will be given below. The general procedure is to fit the experimentally-determined population decay or survival probability, $P(t)$, with multiple exponential decays with different rate constants, k_i , and amplitude, a_i ,

$$P(t) = \sum_i a_i \exp(-k_i t). \quad (1)$$

The decay rate constant can also have a continuous distribution:

$$P(t) = \int_0^\infty \tilde{P}(k) \exp(-kt) dk, \quad (2)$$

with the probability density of decay components, $\tilde{P}(k)$, being the inverse Laplace transform of $P(t)$,

$$\tilde{P}(k) = L^{-1}\{P(t)\} = \frac{1}{2\pi} \int_{b-i\infty}^{b+i\infty} P(t) e^{kt} dt. \quad (3)$$

In principle, $\tilde{P}(k)$ is deducible from $P(t)$. For example, the $\tilde{P}(k)$ for the stretched exponential $P(t)$ is known.³⁴ In practice, however, $\tilde{P}(k)$ cannot be accurately computed from discrete experimental data of $P(t)$ because of the numerical instability of the inverse Laplace transform,³⁵ i.e., a small error in $P(t)$ results in a large error in $\tilde{P}(k)$. As an alternative, the maximum entropy method (MEM) has been used to determine the $\tilde{P}(k)$ from ensemble-averaged decay data.³⁶ Whereas MEM provides better estimates of exponential components and their amplitudes, it does not provide accurate and unique distributions of the rates.

What is implied in Eqs. (1) and (2) is a static distribution or a slow interconversion among the states with different rate constants. For two conformational states with decay rate constants, k_1 and k_2 , the total population is a double exponential decay

$$P_0(t) = a_1 \exp(-k_1 t) + a_2 \exp(-k_2 t), \quad (4)$$

where a_1 and a_2 are the fraction of the two states. Now let us introduce the interconversion between the two states, with a rate constant v , and discuss its effect on Eq. (4):



By solving the master equation for the kinetic scheme in Eq. (5) using matrix algebra,³⁷ the total population decay is still a double exponential decay,

$$P(t) = \chi_+ \exp(-\kappa_+ t) + \chi_- \exp(-\kappa_- t) \quad (6)$$

with the two rate constants (eigenvalues) being

$$\kappa_{\pm} = \frac{1}{2}(k_1 + k_2 + 2v \pm \sqrt{k_1^2 - 2k_1 k_2 + k_2^2 + 4v^2}), \quad (7)$$

and the two amplitudes, χ_+ and χ_- , dependent on a_1 and a_2 at time zero.

Figure 1 shows how κ_+ , κ_- , χ_+ and χ_- change as a function of v , assuming $k_1 = 1$, $k_2 = 10$, $a_1 = a_2 = 0.5$. When $v \gg k_1, k_2$, $\kappa_- = (k_1 + k_2)/2$, and $\kappa_+ = 2v$. Interestingly, χ_+ , the amplitude of the faster component, approaches zero with increasing v . Therefore, $P(t)$ becomes a single exponential, with a decay constant being the mean of k_1 and k_2 at large v . This is similar to the motional narrowing phenomenon of spectral line shapes.^{38,39} Such “motional narrowing” exists for fast interconversion not only between two states but also among multiple or continuous distribution of states.

Here we stress several points: First, $P(t)$ can be meaningfully decomposed to sum or distribution of exponential decays of individual states [Eqs. (1), (2)] only when interconversion among states is much slower than the individual decay rate constants. Second, it is practically impossible to extract the interconversion dynamics from $P(t)$. For example, one cannot determine if a double exponential decay is due to two static states [Eq. (4)] or two interchanging states

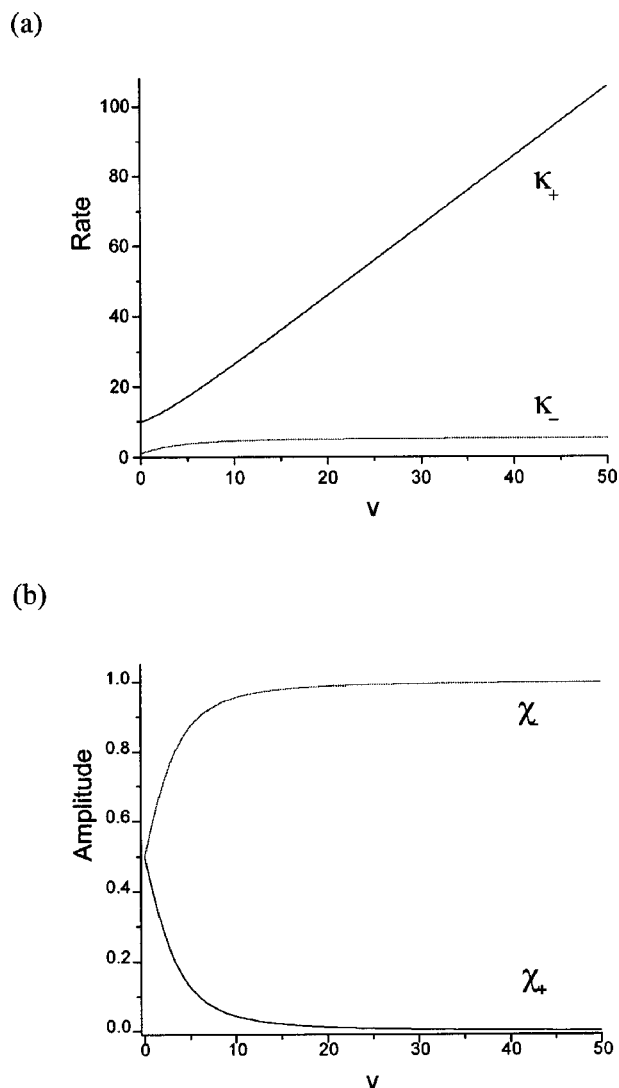


FIG. 1. The effect of motional narrowing. For the kinetic scheme of Eq. (5) the total population decay is a biexponential decay, $P(t) = \chi_+ \exp(-\kappa_+ t) + \chi_- \exp(-\kappa_- t)$. κ_+ and κ_- (a) χ_+ and χ_- (b) are plotted as functions of ν , assuming $k_1 = 10$, $k_2 = 1$, $a_1 = a_2 = 0.5$ in Eqs. (4) and (5). When $\nu = 0$ (static disorder), κ_+ and κ_- are k_1 and k_2 , respectively. With increasing ν , the amplitude (χ_+) of the faster component ($\kappa_+ \rightarrow 2\nu$) approaches zero and $P(t)$ becomes a single exponential decay with the rate constant (κ_-) approaching the mean of k_1 and k_2 .

[Eq. (6)]. Finally, even an apparent single exponential decay can arise from fast interconversion among states of vastly different decay rate constants.

In summary, there are two difficulties associated with knowing only the population decay $P(t)$. First, it is practically impossible to determine the distribution of rate constants from an experimentally-determined $P(t)$. Second, it is impossible to distinguish static heterogeneity from dynamic fluctuation of the decay rate constant. Single-molecule measurements provide not only the distribution of the rates but also the dynamics of interconversion within the distribution. Below, we give two examples in the context of conformational and enzymatic dynamics, respectively. The methodology is generally applicable to other processes.

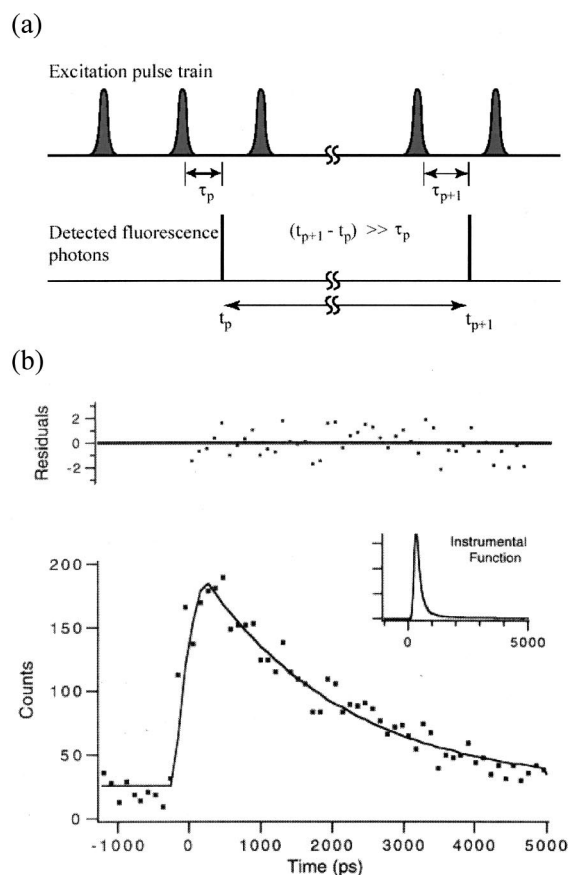


FIG. 2. (a) Schematic of a train of laser excitation pulses and detected fluorescence photons. A histogram of photon delay time, τ_p , is compiled in a time-correlated single-photon counting experiment. (b) Fluorescence decay of a single sulforhodamine 101 molecule on a glass surface. The decay is best fit with a single exponential (2.0 ns) convoluted with the instrument response (inset). The weighted residuals are shown above. (Adapted from Ref. 41.)

III. CONFORMATIONAL DYNAMICS

Fluorescence decay is a good probe for the local environment of a fluorophore, and is usually measured with the time-correlated single-photon counting method,⁴⁰ by which a train of high-repetition laser pulses excites the sample. For each detected photon, one measures the delay time with respect to its excitation pulse [Fig. 2(a)]. Then one can compile a histogram of the delay times [Fig. 2(b)], which is the convolution of $P(t)$ with an instrumental response function. This method works for both ensemble-averaged and single-molecule experiments. Figure 2(b) depicts such a histogram of a single dye molecule,⁴¹ reported shortly after Eric Betzig's seminal demonstration of single-molecule imaging at room temperature with near-field microscopy.⁴² The decay was single exponential, which indicates either no fluctuation of the fluorescence decay rate constant or much faster fluctuation than the fluorescence decay (motionally narrowed). Multiexponential decays of single molecules were subsequently reported^{43–45} indicating conformational fluctuation at a time scale longer than the fluorescence decays.

Figure 3 shows the multiexponential decay of a single natural fluorophore, flavin adenine dinucleotide (FAD), in the binding pocket of an enzyme molecule, flavin:NADH

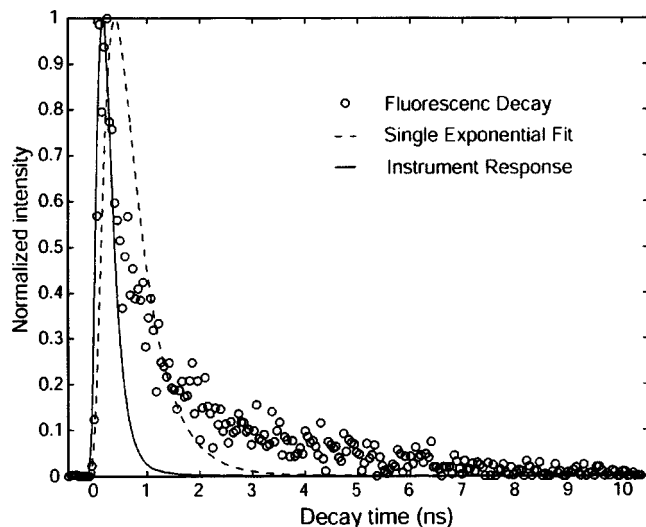


FIG. 3. Fluorescence decay (histogram of τ_p) for a single Fre/FAD complex. The decay is multiexponential, as indicated by a poor fit with a single exponential decay (dashed line). Also shown is the instrumental response function. See Ref. 20 for experimental details.

oxidoreductase (Fre). The single-molecule decay is similar to the ensemble-averaged decay, which is best fit by MEM with four components, ~ 0.03 (25%), 0.20 (52%), ~ 0.45 (21%) and ~ 3.1 ns (1.2%). The distribution of decay rate constants, for reasons described above, cannot be deduced from either the ensemble-averaged or the single-molecule histograms. The multiexponential decay of the single molecule points to the fact that the fluorescence decay rate constant fluctuates during the course of measurements. However, the histogram cannot tell how fast the decay rate constant fluctuates with time, which can be extracted from the single-molecule trajectory. The easiest analysis is the autocorrelation function of k^{-1} fluctuation,

$$C(t) = \langle \Delta k(0)^{-1} \Delta k(t)^{-1} \rangle, \quad (8)$$

where $\Delta k(t)^{-1} = k(t)^{-1} - \langle k^{-1} \rangle$, and the bracket indicates time average. $C(0)$ gives the variance. The decay of $C(t)$ gives the time scale of the fluctuation, i.e., the memory time.

The fluorescence decay rate constant of a fluorophore is affected by the presence of a quencher either through fluorescence energy transfer (FRET)⁴⁶ or electron transfer (ET)²⁰. In this way, the lifetime serves as a distance-dependent probe for conformation fluctuation. The FRET rate constant is dependent on the center-to-center distance between the donor (fluorophore) and acceptor (quencher) to the inverse sixth power, and is sensitive to motions on the order of Förster radius, usually a few nanometers. FRET has found a broad range of applications in studies of conformational dynamics. While ET in biological systems has been extensively studied,⁴⁸ the use of ET in conformational analyses²⁰ is yet to be fully explored. ET rate constants have an exponential dependence on the edge-to-edge distance between the donor and acceptor, and are sensitive to motions on the angstrom scale. We thus have

$$k(t) = k_0 e^{-\beta x(t)}, \quad (9)$$

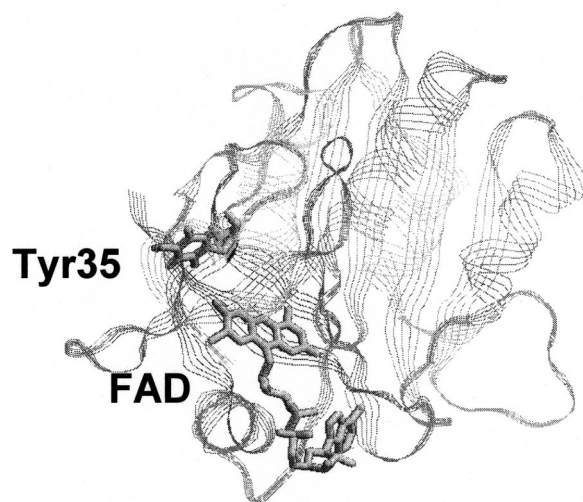


FIG. 4. Structure of the Fre/FAD complex based on M. Ingelman, S. Ramaswamy, V. Nivière, M. Fontecave, and H. Eklund [Biochemistry **38**, 7040 (1999)]. Natural fluorescence from the flavin ring of FAD is quenched by the nearby Tyr35 residue through excited-state electron transfer. The ET rate is used to probe fluctuation of the edge-to-edge distance, x , between the donor (tyrosine) and acceptor (flavin ring).

where $\beta \sim 1.0 - 1.4 \text{ \AA}^{-1}$ for proteins.⁴⁹⁻⁵¹ Although the k fluctuation might be induced by orientation and energetics fluctuations, it is most sensitive to distance fluctuation because of the exponential dependence.²⁰ For example, the fast fluorescence quenching in Fig. 3 is dominated by ET from a nearby tyrosine residue (donor) to the flavin fluorophore (acceptor). The positions of the ET donor and acceptor in the 26 kD protein is shown in Fig. 4.²⁰

Before we present the experimentally measured correlation functions, let's consider two simple models of rate constant fluctuation. First, a two-state model assumes two conformers with different lifetimes, k_1^{-1} and k_2^{-1} , and interconversion rate constants of v_{12} and v_{21} between them. It can be shown that the correlation function of fluorescence lifetime is:⁵²

$$C(t) = \frac{(k_1^{-1} - k_2^{-1})^2 v_{12} v_{21}}{(v_{12} + v_{21})^2} \exp[-(v_{12} + v_{21})t]. \quad (10)$$

This model describes the behavior of dynamic equilibrium between the two states. It corresponds to thermally-activated barrier crossing between the potential wells of two conformational states.

The second model is the Brownian diffusion model, which deals with a continuous distribution of rather than discrete decay rate constants. The fluctuation donor-acceptor distance, x , can be modeled as Brownian diffusion within a harmonic well using the Langevin equation:⁵³

$$\mu \frac{d^2 x}{dt^2} = -\mu \omega^2 (x - x_{eq}) - \eta \frac{dx}{dt} + F(t), \quad (11)$$

where μ is the reduced mass, a harmonic well $V(x) = \frac{1}{2} \mu \omega^2 (x - x_{eq})^2$ is located at the equilibrium position x_{eq} , η is the friction coefficient, and $F(t)$ is the random fluctuating force. Under the overdamped condition, the acceleration (left side) is zero, so Eq. (11) becomes²¹

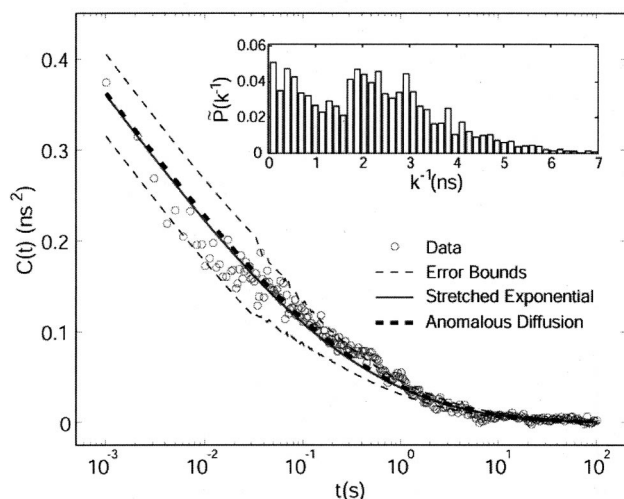


FIG. 5. Autocorrelation function of fluorescence lifetime fluctuation, $C(t)$, of the same Fre/FAD complex as in Fig. 3, plotted in logarithmic scale in time. The data is fit with a stretched exponential decay, $\exp[-(t/\tau_0)^\gamma]$, with $\gamma=0.17$, and $\tau_0=1.4$ ms. The $C(t)$ unravels protein conformational fluctuation spanning a broad range of time scales. The $C(t)$ also fits well with the anomalous diffusion model [Eq. (16)]. Inset: Distribution of fluorescence lifetimes of the same single Fre/FAD complex.

$$\frac{dx}{dt} = -\lambda(x - x_{\text{eq}}) + f(t), \quad (12)$$

where λ is the drifting coefficient, $\lambda = \mu\omega^2/\eta$, and the random variable $f(t) = F(t)/\eta$ is assumed to be white noise with mean $\langle f(t) \rangle = 0$. The fluctuation dissipation theorem⁵³ relates the fluctuation of $f(t)$ with λ such that

$$\langle f(t)f(t') \rangle = 2\lambda\theta\delta(t-t'), \quad (13)$$

where $\theta = \langle \Delta x^2 \rangle = k_B T / \mu\omega^2$, k_B is the Boltzmann constant. It follows that the autocorrelation of x is

$$\langle \Delta x(0)\Delta x(t) \rangle = \theta e^{-\lambda t}. \quad (14)$$

In the time-correlated single-photon counting experiment, we do not measure $x(t)$ directly, but stochastic realization of k . The correlation function of k^{-1} is easier to obtain and less noisy than that of $x(t)$.⁴⁷ We have shown that the autocorrelation function of k^{-1} associated with ET is

$$\begin{aligned} C(t) &= \langle \Delta k(t)^{-1} \Delta k(0)^{-1} \rangle \\ &= k_0^{-2} \exp(2\beta x_{\text{eq}} + \beta^2 \theta) [-1 + \exp(\beta^2 \theta e^{-\lambda t})]. \end{aligned} \quad (15)$$

Note that Eqs. (14) and (15) are characterized by a single time scale λ^{-1} .

In a single-molecule experiment, we cannot determine the $k(t)$ at a particular moment of time because of the stochastic arrival times of individual photons. The conventional method is to bin detected photons in long time intervals. The drawback is that it sacrifices the time resolution and limits the range of accessible time scales given a finite number of detectable photons before photobleaching of the fluorophore. In the article by Yang *et al.* in this issue,⁴⁷ we present a new method analyzing lifetime trajectories on a photon-by-photon basis, which not only improves the time resolution of

$C(t)$ but also extends the detectable time scales to a broader range. In order to have high time resolution, we need short bins. The uncertainty in each bin is increased. However, the uncorrelated fluctuation in different time bins will only contribute to the variance, $C(0)$, but not to $C(t)$ beyond zero time. With this method, time resolution of the $C(t)$ can be as high as one over the photon count rate.⁴⁷ In principle, sub-microsecond time resolution is possible, allowing direct comparison between MD simulations and single-molecule experiments in the future.

Shown in Fig. 5 is the $C(t)$ of an FAD/Fre complex in linear logarithm scale, which was obtained with the photon-by-photon method.²⁰ This is an interesting result in regard to the dynamical properties of proteins. If there were no distance fluctuation, $C(t)$ would be a spike only at time zero. Instead, the decay of $C(t)$ spans four decades of time scales, reflecting conformational changes, fluctuation of x in particular, occurring from 1 ms to 10 s. The $C(t)$ in Fig. 5 can be fit well with a stretched exponential, $\exp[-(t/\tau_0)^\gamma]$, with $\gamma=0.17$ and $\tau_0=1.4$ ms.

The time scale of fluctuation at room temperature is rather long, so much so that some people were surprised by its existence. In an ensemble-averaged study of conformational changes of myoglobin after photodissociation of a bound ligand, stretched exponential kinetics of conformational relaxation ranging from picosecond to microsecond time scale was observed at room temperature.²⁵ This was probed with a near infrared spectral transition of the heme, which is highly sensitive to the protein environment. However, as discussed earlier, the ensemble-averaged measurement could not distinguish dynamic disorder from static disorder. Our measured $C(t)$ provides a direct measurement of the interconversion among the conformers at an even longer time scale (100 μs –10 s) for a protein smaller than myoglobin.

An important distinction between our single-molecule experiment and the previous ensemble-averaged photodissociation experiments^{22–25} is that our experiment probes equilibrium fluctuation. In contrast, the previous experiments probed nonequilibrium relaxation. Although photoexcitation of the fluorophore in our experiment leads to electron transfer on the excited state, the back transfer completes within a few nanoseconds such that both donor and acceptor return to their original states. The $C(t)$ is independent of excitation intensity, indicating the observed fluctuation originated from the spontaneous fluctuation of the ground electronic state, rather than photoinduced processes.²⁰ Although nuclear magnetic resonance spectroscopy is capable of probing spontaneous motions from microsecond to millisecond time scale,⁵⁴ it is also an ensemble-averaged experiment.

In addition to $C(t)$, we can determine the distribution of k by constructing a histogram of k measured in fixed time intervals (course grained), as shown in Fig. 5. The potential of mean force, can be experimentally determined by $V(x) = -k_B T \ln p(x)$. $p(x)$ is the probability density of x for the entire trajectory, mapped from $\tilde{P}(k)$, and is shown in Fig. 6. The bottom of the potential of mean force is near harmonic.

The stretched exponential $C(t)$ cannot be explained by the two-state or Brownian diffusion model discussed above.

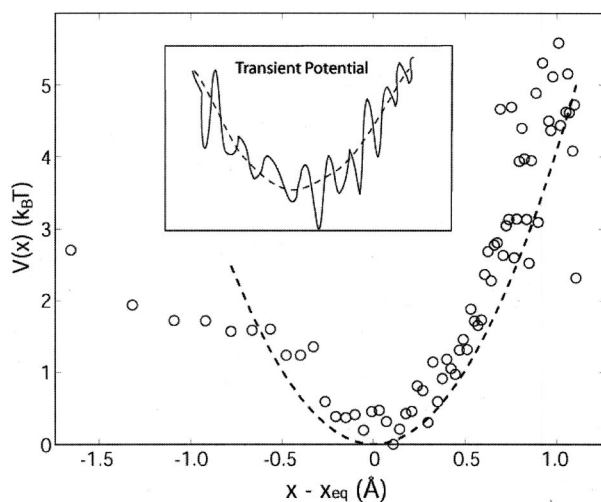


FIG. 6. Potential of mean force calculated from the lifetime trajectory of the same Fre/FAD complex as in Fig. 3 and 5. The dashed line is a fit to a harmonic potential of mean force, $V_0(x) = k_B T(x - x_{eq})^2 / 2\theta$. T is 300 K and $\theta = 0.13 \text{ \AA}^2$. Inset: A sketch of a rugged transient potential that has a distribution of fluctuating barrier heights.

It points to the existence of multiple conformational states at a wide range of time scales, which is consistent with the energy landscape picture popularized by Hans Frauenfelder.⁵⁵ According to this picture, conformational states correspond to the minima of multidimensional potential energy surfaces. This intuition resulted from extensive ensemble-averaged experiments on recombination kinetics of photodissociated ligands in heme proteins.²³ At low temperatures, the recombination kinetics is highly dispersed because of static heterogeneity of the conformal states. At elevated temperatures, the kinetics becomes less dispersed (motionally narrowed) because of interconversion among the conformational states. Current computational approaches can calculate the free energies of the conformational states, e.g., the local minima; those within a few $k_B T$ will be populated significantly. However, it is a difficult task to compute the barrier heights connecting the local minima, some promising methodology notwithstanding.^{56–59} There are small barriers and large barriers. Assuming an Arrhenius process with a prefactor of 10^{12} s^{-1} , if a barrier height is 0.5 kcal/mol, a conformational transition takes place on the picosecond time scale; if a barrier height is 16 kcal/mol, a conformational transition takes place on the second time scale.

The experimentally accessible one-dimensional (1D) coordinate, x , varies as the three dimensional structure of the protein/flavin complex changes. The projection of the multidimensional potential to the x coordinate gives fluctuating 1D potential. Its short time average is the “transient potential” depicted in the inset of Fig. 6, which is a rugged function of x . The barrier height for escaping a particular x has a broad distribution, which is associated with the broad range of survival times for the three-dimensional (3D) conformational states with the particular x . The long-time average of the transient potential is the smooth potential of mean force. The single-molecule trajectories provide much richer information regarding the properties of the energy landscape and the dynamics within than previous ensemble experiments.

Our data indicated that the trapping time at a particular x can be rather long, resulting from the metastable 3D structures trapped in deep potential wells. The stretched exponential $C(t)$ cannot be explained by the Brownian diffusion model [Eq. (15)]. This is because the model implies a distribution of trapping time (τ) at a particular x with a finite mean. For example, the finite mean can be the time constant of an exponential τ distribution associated with equal barrier heights in the 1D potential. In contrast, there might be a power law distribution of the trapping time, $1/\tau^{1+\alpha}$, $0 < \alpha < 1$, which has no finite first moment. This might arise from a distribution of the fluctuating barrier height in the rugged 1D potential. This is the subdiffusion regime of anomalous diffusion, in which the mean square displacement is $\langle \Delta x^2 \rangle \propto t^\alpha$, in the absence of bound potential, $V(x) = 0$. Anomalous diffusion has been extensively studied⁶⁰ and has been used to address protein motion.⁶¹ Recently, Klafter and co-workers developed a theory to describe subdiffusive motion within a potential based on a fractional Fokker–Planck equation (FFPE).⁶² Taking $V_0(R) = k_B T(x - x_{eq})^2 / 2\theta$ as the potential (Fig. 6), we solved the FFPE for $C(t)$,⁴⁷

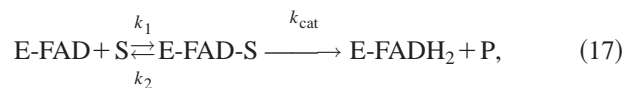
$$C(t) = k_0^{-2} \exp(2\beta x_{eq} + \beta^2 \theta) [\exp(\beta^2 \theta e^{-\eta_\alpha t^\alpha / \Gamma(1+\alpha)}) - 1], \quad (16)$$

where η_α is the generalized drift coefficient and has a fractional unit of $\text{s}^{-\alpha}$, and $\Gamma(z) = \int_0^\infty y^{z-1} e^{-y} dy$ is the gamma function. As shown in Fig. 5, Eq. (16) fits the experimental data extremely well,²⁰ with $\alpha = 0.17$ and $\eta_\alpha = 2.9 \text{ s}^{-\alpha}$. Although other theoretical models, such as spin glass model^{63–66} might also account for the observation, the advantage of the FFPE approach is that it provides a simple physical picture and has only two adjustable parameters.

The microscopic picture of the conformational states is not yet known. The nature of the barriers is a subject of our current investigation. The barrier heights among the conformational states are significant, but not unphysically high, and are comparable to breaking and reforming a few hydrogen bonds. The power law distribution of the trapping time arises from an exponential distribution of the barrier heights.^{23,67} The existence of large barrier heights results in conformational fluctuation at the time scale of enzymatic reactions. What is the implication of the phenomenon to enzymatic dynamics?

IV. ENZYMATIC DYNAMICS

In 1998, Lu *et al.* made an observation that the enzymatic turnover rate of a single enzyme molecule fluctuates at the time scale comparable to the enzymatic reaction, and attributed the fluctuation to conformational changes.¹² The enzyme is cholesterol oxidase (COx). The active site of the enzyme involves a tightly-bound FAD. Cholesterol is oxidized to cholesterone by the FAD via the Michaelis–Menten mechanism:



FADH₂ in the enzyme is then oxidized by oxygen to regenerate FAD.

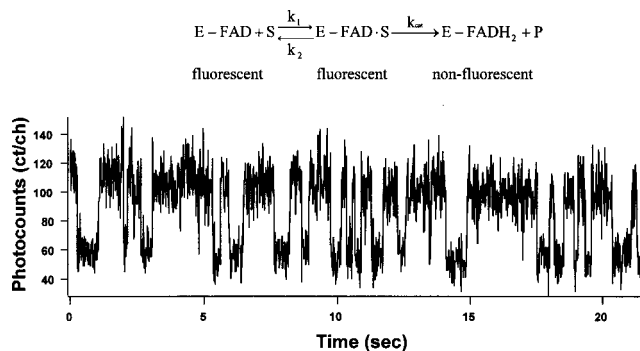


FIG. 7. Real-time observation of enzymatic turnovers of a single cholesterol oxidase (COx) molecule catalyzing oxidation of cholesterol molecules by oxygen. The emission from a single COx molecule as a function of time is plotted. Each on-off cycle in the emission intensity trajectory corresponds to an enzymatic turnover. The Michaelis-Menten mechanism of the enzymatic reaction is shown in the inset. (Adapted from Ref. 12.)



As shown in Fig. 7, fluorescence of a single enzyme molecule turns on and off as the FAD switches between the oxidized (fluorescent) and reduced (nonfluorescent) states, respectively. Each on-off cycle corresponds to an enzymatic turnover. The stochastic emission on-times (τ) correspond to the “waiting times” for the FAD reduction reaction [Eq. (17)] to complete.

We now consider the situation when k_{cat} is rate-limiting (at saturating substrate concentration). The population decay of the Michaelis-Menten complex, E-FAD·S, in an ensemble-averaged (e.g., stop-flow) experiment corresponds to $P(\tau)$, the probability density of τ in our single-molecule experiment. $P(\tau)$ is experimentally measured by constructing the histogram of τ . In the absence of dynamic disorder, $P(\tau)$ is a single exponential function, $P(\tau) = k_{\text{cat}} \exp(-k_{\text{cat}}\tau)$. The histogram in Fig. 8 appears to be single exponential decay, though the statistics are not good enough to distinguish single or multiexponential distributions. Is there dynamics disorder of k_{cat} , similar to Eq. (5)? As discussed before, if interconversion rate constants among conforma-

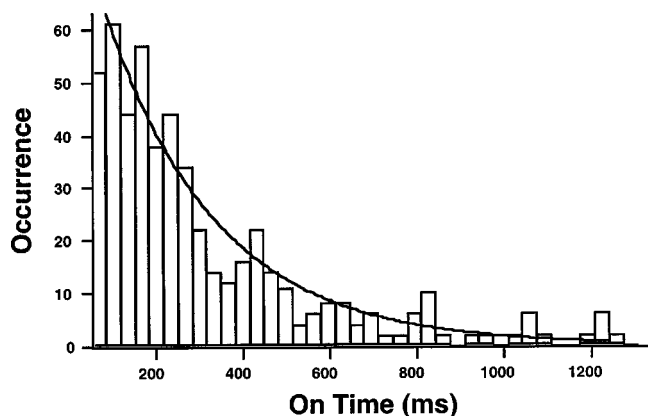


FIG. 8. Histogram of the on-times of a COx fluorescence intensity trajectory taken at a high substrate concentration at which k_{cat} is rate-limiting. The solid line is a single exponential fit with $k_2 = 3.9 \pm 0.5 \text{ s}^{-1}$. (Adapted from Ref. 12.)

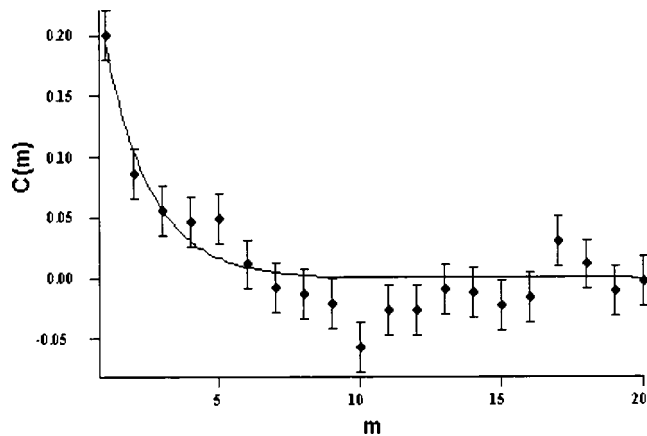


FIG. 9. Autocorrelation function of the on-times for the same trajectory as in Fig. 8. $C(m) = \langle \Delta\tau(0)\Delta\tau(m) \rangle / \langle \Delta\tau^2 \rangle$, m being the index numbers of turnovers. $\Delta\tau(m) = \tau(m) - \langle \tau \rangle$. The fact that $C(m)$ is not simply a spike at $m=0$ indicates dynamic disorder of k_{cat} . The time constant of the decay gives the timescale of the k_{cat} fluctuation. (Adapted from Ref. 12.)

tional states of different k_{cat} are much faster than k_{cat} , $P(\tau)$ should be a single exponential with the decay rate constant being the average of k_{cat} of all conformational states. For slow interconversion, $P(\tau)$ should be a multiexponential distribution. However, $P(\tau)$ contains no information on interconversion rate constants.

A much more sensitive way to evaluate the dynamic disorder is the autocorrelation function of τ ,

$$C(m) = \langle \Delta\tau(0)\Delta\tau(m) \rangle / \langle \Delta\tau^2 \rangle = \frac{\sum_i \Delta\tau(i)\Delta\tau(i+m)}{\sum_i \Delta\tau^2(i)}, \quad (19)$$

where m is the index number for the turnovers and $\Delta\tau(m) = \tau(m) - \langle \tau \rangle$, with the bracket denoting the average along the trajectory. In the absence of dynamic disorder, $C(0) = 1$ and $C(m) = 0 (m > 0)$. In the presence of dynamic disorder, $C(m)$ decays at the timescale of interconversion from the initial ($m=1$) amplitude, which reflects the variance of the rate constant among different conformations.

Figure 9 shows the $C(m)$ derived from a single-molecule trajectory of cholesterol oxidase with saturating concentration of substrate. The decay constant is $1.0 \pm 0.3 \text{ s}$. Dynamic disorder of k_{cat} is evident. The dynamic disorder is not apparent from the seemingly single exponential histogram in Fig. 8 because of motional narrowing. Assuming there are two conformers with different values of k_{cat} , they have to differ by at least a factor of 10 in order to account for the $C(m)$.⁶⁸ This is obviously not a small effect. A Brownian diffusion model also fits the data well.⁶⁸ In light of the new experiment summarized above, an anomalous diffusion description involving a broad distribution of conformations might be more appropriate. However, we do not yet know whether the $C(m)$ in Fig. 9 is a single exponential or a stretched exponential decay because of noise associated with the limited length of the trajectory.

Single-molecule studies of dynamic disorder have been the subject of an increasing amount of theoretical work,^{47,52,68-76} Several theoretical investigations have been focused on the cholesterol oxidase experiment, with some

dealing with discrete conformational states^{68,73,75} and others using Brownian diffusion models.^{68,74} It is interesting to note that recent theoretical work on single-molecule enzymology emphasizes the effect of energetics on the nonequilibrium nature of enzymatic reactions.^{77,78}

Are there any fluctuations of conformation and enzymatic activity at even longer time scales? A single-molecule enzymatic assay pioneered by Yeung's group has revealed static disorder in enzymatic turnover rates of pure enzyme molecules.⁷⁹ In a capillary tube containing a solution of highly diluted enzyme molecules of lactate dehydrogenase, and concentrated substrate molecules (lactate and nicotinamide adenine dinucleotide, NAD⁺), each enzyme molecule produced a discrete zone of thousands of NADH molecules after 1 hour of incubation. The zones were then eluted by capillary electrophoresis and monitored by natural fluorescence of NADH. The enzyme molecules had a broad distribution of activity. The heterogeneity was found to be static at the hour time scale because the same enzyme molecule produces the same zone intensity after another incubation period. The heterogeneity was also independent of the position of the enzyme molecule in the capillary tube. The origin of the static disorder was attributed to different conformers, which is not inconsistent with the fact there exist extremely large barriers between the conformers. Dovichi and co-workers have used a similar approach to study calf intestinal alkaline phosphatase and found an even broader, multipeak distribution of activities.⁸⁰ This static disorder was attributed to glycosylation and other post-translational modifications, which produce nonidentical copies of the enzyme. Of course, one would want to do single-molecule experiments with pure samples of "identical" copies of molecules. Dovichi's group has recently examined bacterial alkaline phosphatase and found no variation on the hour-long time scale.⁸¹ While Yeung's lactate dehydrogenase was also electrophoretically pure, the existence of the variations of k_{cat} on the hour-long timescale remains to be tested on other systems. We note a similar long-time memory effect has also been observed on single ribozyme molecules.⁸² Ergodicity is dependent on the time scale of the measurement. If extremely high barriers exist, even identical single molecules could exhibit an apparent static distribution on the hour-long scale. Suffice to say that the conformational fluctuation and dynamic disorder of enzymatic reaction on the subsecond time scales existed for every enzyme molecule that we studied in the Fre and COx systems.

We expect the dynamic disorder to be a general phenomenon in enzymology, which has been otherwise masked in ensemble-averaged measurements. Similar slow enzymatic rate changes have been inferred previously from other monomeric enzyme systems, and hypothesized to be relevant to physiological enzymatic regulation.^{83–85} In any case, the availability of conformations with different enzymatic rates opens up possibilities for control. If nature really takes advantage of or even orchestrated the dynamic disorder, the evolution consequence poses an interesting question. Regardless of whether the hypothesis is true or not, the single-molecule approach allowed us to ask and to tackle this question. The physiological relevance of the dynamic disorder

phenomenon, if any, will be best investigated by single-molecule experiments in cellular environments, which are currently being pursued in many laboratories.

V. SUMMARY

We have given a perspective of the single-molecule approach to conformational and enzymatic dynamics. The single-molecule approach is extremely useful in studying dispersed kinetics and dynamic disorder. In particular, fluorescence lifetime experiments of natural fluorophores quenched by electron transfer reactions yielded new dynamic information previously unavailable. Our single-molecule experiments have provided the picture and added quantitative understanding that an enzyme molecule is a dynamic entity with conformational fluctuation spanning a vast range of time scales. The slow conformational changes lead to fluctuations of biochemical reactivity. Further studies of the conformational and enzymatic dynamic with the single-molecule approach will shed light on how enzyme work at a level of great details.

ACKNOWLEDGMENTS

The author thanks current and former members of my research group, particularly Haw Yang, Peter Lu, Guobin Luo, and Long Cai, for their contributions to the work summarized here. Our work in this area has benefited from collaborations and interactions with many colleagues, in particular, Luying Xun, Martin Karplus, Yossi Klafter, Gregory Schenter, Samuel Kou, Jun Liu, David Reichman, Eugene Shakhnovich and Ioan Andricioaei. The work is funded by National Institute of Health and Department of Energy.

¹H. Gutfreund and J. R. Knowles, in *Essays Biochem.* **3**, 25 (1967).

²See Plate 626, "Annie G." galloping, Eadweard Muybridge, *Muybridge's Complete Human and Animal Locomotion: New Volume 1*, Anita V. Mozley, designer (Dover, New York, 1979).

³For an overview, see articles in *Femtochemistry and Femtobiology: Ultrafast Reaction Dynamics at Atomic-Scale Resolution, Nobel Symposium 101*, edited by V. Sundstrom (Imperial College Press, London, 1997).

⁴For an overview, see the special issue on molecular dynamics simulation, edited by M. Karplus, *Acc. Chem. Res.* **35**, 321 (2002).

⁵Y. Duan and P. A. Kollman, *Science* **282**, 740 (1998).

⁶A. Warshel, *Acc. Chem. Res.* **35**, 385 (2002).

⁷D. Chandler, in *Introduction to Modern Statistical Mechanics* (Oxford University Press, Oxford, 1987), Ch. 8.

⁸E. Neria and M. Karplus, *Chem. Phys. Lett.* **267**, 23 (1997).

⁹R. Yasuda, H. Noji, K. Kinoshita, and M. Yoshida, *Cell* **93**, 1117 (1998); R. Yasuda, H. Noji, M. Yoshida, K. Kinoshita, and H. Itoh, *Nature (London)* **410**, 898 (2001).

¹⁰T. Funatsu, Y. Harada, M. Tokunaga, K. Saito, and T. Yanagida, *Nature (London)* **374**, 555 (1995).

¹¹M. J. Schnitzer and S. M. Block, *Nature (London)* **388**, 386 (1997); M. Wang, M. S. Schnitzer, H. Yin, R. Landick, J. Gelles, and S. M. Block, *Science* **282**, 902 (1998).

¹²H. P. Lu, L. Xun, and X. S. Xie, *Science* **282**, 1877 (1998); X. S. Xie and H. P. Lu, *J. Biol. Chem.* **274**, 15967 (1999).

¹³G. J. L. Wuite, S. B. Smith, M. Young, D. Keller, and C. Bustamante, *Nature (London)* **404**, 103 (2000).

¹⁴X. Zhuang, L. E. Bartley, H. P. Babcock, R. Russell, T. Ha, D. Herschlag, and S. Chu, *Science* **288**, 2048 (2000).

¹⁵T. Strick, J. F. Allemand, V. Croquette, and D. Bensimon, *Phys. Today* **54**, 46 (2001).

¹⁶H. Yin, I. Artsimovitch, R. Landick, and J. Gelles, *PNAS* **96**, 13124 (1999); K. M. Dohoney and J. Gelles, *Nature (London)* **409**, 370 (2001).

- ¹⁷H. Sosa, E. J. G. Peterman, W. E. Moerner, and L. S. B. Goldstein, *Nat. Struct. Biol.* **8**, 540 (2001).
- ¹⁸X. S. Xie, *Single Molecules* **2**, 229 (2001).
- ¹⁹S. Weiss, *Science* **283**, 1676 (1999).
- ²⁰H. Yang, G. Luo, P. Karnchanaphanurach, T.-M. Louie, L. Xun, and X. S. Xie (preprint) (2002).
- ²¹R. Zwanzig, *Acc. Chem. Res.* **23**, 148 (1990).
- ²²H. Frauenfelder, F. Parak, and R. D. Young, *Annu. Rev. Biophys. Biophys. Chem.* **17**, 451 (1988).
- ²³R. Austin, K. W. Beeson, L. Eisenstein, and H. Frauenfelder, *Biochemistry* **14**, 5355 (1975).
- ²⁴J. W. Petrich, J.-C. Lambry, K. Kuczera, M. Karplus, C. Poyart, and J.-L. Martin, *Biochemistry* **30**, 3975 (1991); K. Kuczera, J.-C. Lambry, J.-L. Martin, and M. Karplus, *Proc. Natl. Acad. Sci. U.S.A.* **90**, 5805 (1993).
- ²⁵M. Lim, T. A. Jackson, and P. A. Anfinsen, *Proc. Natl. Acad. Sci. U.S.A.* **90**, 5801 (1993); T. A. Jackson, M. Lim, and P. A. Anfinsen, *Chem. Phys.* **180**, 131 (1994); S. Hagen and W. A. Eaton, *J. Chem. Phys.* **104**, 3395 (1996).
- ²⁶K. Rubinson, *Biophys. J.* **61**, 463 (1992).
- ²⁷S. M. Bezrukov and M. Winterhalter, *Phys. Rev. Lett.* **85**, 202 (2000).
- ²⁸B. Sakamann and E. Neher, in *Single-Channel Recording*, 2nd ed. (Plenum, New York, 1995).
- ²⁹F. Kohlrausch, *Pogg. Ann. Phys.* **119**, 352 (1863).
- ³⁰G. Williams and D. C. Watts, *Trans. Faraday Soc.* **66**, 80 (1970).
- ³¹H. Scher, M. F. Shlesinger, and J. T. Blendler, *Phys. Today* **44**, 26 (1991).
- ³²J. Ross and M. Vlad, *Annu. Rev. Phys. Chem.* **50**, 51 (1999).
- ³³J. Laherrere and D. Sornette, *Eur. Phys. J. B* **2**, 525 (1998).
- ³⁴For $\gamma=1/2$,
- $$\bar{P}(k) = \frac{1}{2\sqrt{\pi\tau_0}} k^{-3/2} \exp\left(-\frac{1}{4k\tau_0}\right);$$
- for $\gamma \neq 1/2$,
- $$\bar{P}(k) = \int_0^\infty \frac{1}{\pi} \exp\left[-kx - \left(\frac{x}{\tau_0}\right)^\gamma \cos(\gamma\pi)\right] \sin\left[\left(\frac{x}{\tau_0}\right)^\gamma \sin(\gamma\pi)\right] dx.$$
- See L. S. Liebovitch and T. I. Toth, *Bull. Math. Biol.* **53**, 443 (1991); and C. P. Lindsey and G. D. Patterson, *J. Chem. Phys.* **73**, 3348 (1980).
- ³⁵J. G. McWhirter and E. R. Pike, *J. Phys. A* **11**, 1729 (1978).
- ³⁶A. K. Livesey and J. C. Brochon, *Biophys. J.* **52**, 693 (1987); J. C. Brochon, *Methods Enzymol.* **240**, 262 (1994).
- ³⁷N. G. van Kampen, in *Stochastic Processes in Physics and Chemistry* (Elsevier Science, Amsterdam, 1992).
- ³⁸R. Kubo, in *Fluctuation, Relaxation, and Resonance in Magnetic Systems* (Oliver and Boyd, London, 1961), p. 23; R. Kubo, N. Toda, and N. Hashitsume, in *Statistical Physics II* (Springer, Berlin, 1985).
- ³⁹P. W. Anderson, *J. Phys. Soc. Jpn.* **9**, 316 (1954).
- ⁴⁰D. V. O'Connor and D. Phillips, in *Time-Correlated Single Photon Counting* (Academic, Orlando, 1984).
- ⁴¹X. S. Xie and R. C. Dunn, *Science* **265**, 361 (1994).
- ⁴²E. Betzig and R. Chichester, *Science* **262**, 1422 (1993).
- ⁴³L. Edman, U. Mets, and R. Rigler, *Proc. Natl. Acad. Sci. U.S.A.* **93**, 6710 (1996).
- ⁴⁴Y.-W. Jia, A. Sytnik, L. Li, S. Vladimirov, S. Cooperman, and R. M. Hochstrasser, *Proc. Natl. Acad. Sci. U.S.A.* **94**, 7932 (1997).
- ⁴⁵C. Eggeling, J. R. Fries, L. Brand, R. Gunter, and C. A. M. Seidel, *Proc. Natl. Acad. Sci. U.S.A.* **95**, 1556 (1998).
- ⁴⁶L. Stryer, *Annu. Rev. Biochem.* **47**, 819 (1978).
- ⁴⁷H. Yang and X. S. Xie, *J. Chem. Phys.* **117**, 10965 (2002), this issue.
- ⁴⁸For reviews, see R. A. Marcus and N. Sutin, *Biochim. Biophys. Acta* **811**, 265 (1985); J. Jortner and M. Bixon, *Electron Transfer—From Isolated Molecules to Biomolecules*, Vol. 106 (Wiley, New York, 1999).
- ⁴⁹C. C. Moser, J. M. Keske, K. Warncke, R. S. Farid, and P. L. Dutton, *Nature (London)* **355**, 796 (1992).
- ⁵⁰H. B. Gray and J. R. Winkler, *Annu. Rev. Biochem.* **65**, 537 (1996).
- ⁵¹D. N. Beratan and S. S. Skourtis, *Curr. Opin. Chem. Biol.* **2**, 235 (1998).
- ⁵²H. Yang and X. S. Xie, *Chem. Phys.* **284**, 423 (2002).
- ⁵³R. Zwanzig, in *Nonequilibrium Statistical Mechanics* (Oxford University Press, 2001).
- ⁵⁴A. G. Palmer, C. D. Kroenke, and J. P. Loria, *Methods Enzymol.* **339**, 204 (2001); A. G. Palmer, *Annu. Rev. Neurosci.* **30**, 129 (2001).
- ⁵⁵H. Frauenfelder, S. G. Sligar, and P. G. Wolynes, *Science* **254**, 1598 (1991).
- ⁵⁶P. G. Bolhuis, D. Chandler, C. Dellago, and P. L. Geissler, *Annu. Rev. Phys. Chem.* **53**, 291 (2002).
- ⁵⁷R. Elber, A. Ghosh, and A. Cardenas, *Acc. Chem. Res.* **35**, 396 (2002).
- ⁵⁸S. V. Krivov, S. F. Chekmarev, and M. Karplus, *Phys. Rev. Lett.* **88**, 038101 (2002).
- ⁵⁹J. Shimada, E. Kussell, and E. I. Shakhnovich, *J. Mol. Biol.* **308**, 79 (2001).
- ⁶⁰For a review, see J. Klafter, M. F. Shlesinger, and G. Zumofen, *Phys. Today* **49**, 33 (1996).
- ⁶¹A. E. Garcia, R. Blumenfeld, G. Hummer, and J. A. Krumhansl, *Physica D* **107**, 225 (1997).
- ⁶²R. Metzler, E. Barkai, and J. Klafter, *Phys. Rev. Lett.* **82**, 3563 (1999).
- ⁶³J. D. Bryngelson and P. G. Wolynes, *Proc. Natl. Acad. Sci. U.S.A.* **84**, 7524 (1987).
- ⁶⁴E. I. Shakhnovich and A. M. Gutin, *Europhys. Lett.* **9**, 569 (1989).
- ⁶⁵C. L. Lee, C. T. Lin, G. Stell, and J. Wang (preprint).
- ⁶⁶D. Reichman (preprint).
- ⁶⁷A. Blumen, J. Klafter, and G. Zumofen, in *Fractals in Physics*, edited by L. Pietronero and E. Tosatti (1986), p. 399.
- ⁶⁸G. K. Schenter, H. P. Lu, and X. S. Xie, *J. Phys. Chem. A* **103**, 10477 (1999).
- ⁶⁹J. Wang and P. Wolynes, *Phys. Rev. Lett.* **74**, 4317 (1995).
- ⁷⁰J. N. Onuchic, J. Wang, and P. G. Wolynes, *Chem. Phys.* **247**, 175 (1999).
- ⁷¹E. Geva and J. L. Skinner, *Chem. Phys. Lett.* **288**, 225 (1998).
- ⁷²A. M. Berezhkovski, A. Szabo, and G. H. Weiss, *J. Chem. Phys.* **110**, 9145 (1999); A. M. Berezhkovskii, M. Boguna, and G. H. Weiss, *Chem. Phys. Lett.* **336**, 321 (2001).
- ⁷³J. Cao, *Chem. Phys. Lett.* **327**, 38 (2000); S. L. Yang and J. S. Cao, *J. Phys. Chem. B* **105**, 6536 (2001); S. Yang and J. Cao, *J. Chem. Phys.* **117**, 10996 (2002), this issue; **117**, 11010 (2002), this issue.
- ⁷⁴N. Agmon, *J. Phys. Chem. B* **104**, 7830 (2000).
- ⁷⁵G. H. Weiss and J. Masoliver, *Physica (Amsterdam)* **296**, 75 (2001).
- ⁷⁶V. Chernyak, M. Schulz, and S. Mukamel, *J. Chem. Phys.* **111**, 7416 (1999); V. Barsegov, V. Chernyak, and S. Mukamel, *J. Chem. Phys.* **116**, 4240 (2002).
- ⁷⁷D. Astumian, *Appl. Phys. A* **75**, 1 (2002).
- ⁷⁸H. Qian and E. Elson, *Biophys. Chem.* (to be published).
- ⁷⁹Q. F. Xue and E. S. Yeung, *Nature (London)* **373**, 681 (1995).
- ⁸⁰D. B. Craig, E. A. Arriaga, J. C. Y. Wong, H. Lu, and N. J. Dovichi, *J. Am. Chem. Soc.* **118**, 5245 (1996).
- ⁸¹R. Polakowski, D. Craig, A. Skelley, and N. J. Dovichi, *J. Am. Chem. Soc.* **122**, 4853 (2000).
- ⁸²X. Zhuang, H. Kim, M. J. B. Pereira, H. P. Babcock, N. G. Walter, and S. Chu, *Science* **296**, 1473 (2002).
- ⁸³C. Frieden, *Annu. Rev. Biochem.* **48**, 471 (1979).
- ⁸⁴J. Ricard and J. Meunier, *Eur. J. Biochem.* **49**, 195 (1974).
- ⁸⁵K. E. Neet and G. R. Anislie, *Methods Enzymol.* **64**, 192 (1980).